Limnol. Oceanogr., 57(3), 2012, 698–710

doi:10.4319/lo.2012.57.3.0698

The Pacific oyster, *Crassostrea gigas*, shows negative correlation to naturally elevated carbon dioxide levels: Implications for near-term ocean acidification effects

Alan Barton,[a] Burke Hales,[b,*] George G. Waldbusser,[b] Chris Langdon,[c] and Richard A. Feely[d]

[a] Pacific Coast Shellfish Grower's Association, Emerald Isle, North Carolina
[b] College of Oceanic and Atmospheric Sciences, Oregon State University, Corvallis, Oregon
[c] Department of Fisheries and Wildlife and Coastal Marine Experiment Station, Oregon State University, Newport, Oregon
[d] Pacific Marine Environmental Laboratory, National Oceanic and Atmospheric Administration, Seattle, Washington

Abstract

We report results from an oyster hatchery on the Oregon coast, where intake waters experienced variable carbonate chemistry (aragonite saturation state < 0.8 to > 3.2; pH < 7.6 to > 8.2) in the early summer of 2009. Both larval production and midstage growth ($\sim$ 120 to $\sim$ 150 μm) of the oyster *Crassostrea gigas* were significantly negatively correlated with the aragonite saturation state of waters in which larval oysters were spawned and reared for the first 48 h of life. The effects of the initial spawning conditions did not have a significant effect on early-stage growth (growth from D-hinge stage to $\sim$ 120 μm), suggesting a delayed effect of water chemistry on larval development.

Rising atmospheric carbon dioxide (CO_2) driven by anthropogenic emissions has resulted in the addition of over 140 Pg-C (1 Pg = 10^{15} g) to the ocean (Sabine et al. 2011). The thermodynamics of the reactions between carbon dioxide and water require this addition to cause a decline of ocean *p*H and carbonate ion concentrations ($[CO_3^{=}]$). For the observed change between current-day and preindustrial atmospheric CO_2, the surface oceans have lost approximately 16% of their $[CO_3^{=}]$ and decreased in pH by 0.1 unit, although colder surface waters are likely to have experienced a greater effect (Feely et al. 2009). Projections for the open ocean suggest that wide areas, particularly at high latitudes, could reach low enough $[CO_3^{=}]$ levels that dissolution of biogenic carbonate minerals is thermodynamically favored by the end of the century (Feely et al. 2009; Steinacher et al. 2009), with implications for commercially significant higher trophic levels (Aydin et al. 2005).

There is considerable spatial and temporal variability in ocean carbonate chemistry, and there is evidence that these natural variations affect marine biota, with ecological assemblages next to cold-seep high-CO_2 sources having been shown to be distinct from those nearby but less affected by the elevated CO_2 levels (Hall-Spencer et al. 2008). Coastal environments that are subject to upwelling events also experience exposure to elevated CO_2 conditions where deep water enriched by additions of respiratory CO_2 is brought up from depth to the nearshore surface by physical processes. Feely et al. (2008) showed that upwelling on the Pacific coast of central North America markedly increased corrosiveness for calcium carbonate minerals in surface nearshore waters. A small but significant amount of anthropogenic CO_2 present in the upwelled source waters provided enough additional CO_2 to cause widespread corrosiveness on the continental shelves (Feely et al. 2008). Because the source water for upwelling on the North American Pacific coast takes on the order of decades to transit from the point of subduction to the upwelling locales (Feely et al. 2008), this anthropogenic CO_2 was added to the water under a substantially lower-CO_2 atmosphere than today's, and water already en route to this location is likely carrying an increasing burden of anthropogenic CO_2. Understanding the effects of natural variations in CO_2 in these waters on the local fauna is critical for anticipating how more persistently corrosive conditions will affect marine ecosystems.

The responses of organisms to rising CO_2 are potentially numerous and include negative effects on respiration, motility, and fertility (Portner 2008). From a geochemical perspective, however, the easiest process to understand conceptually is that of solid calcium carbonate ($CaCO_{3,s}$) mineral formation. In nearly all ocean surface waters, formation of $CaCO_{3,s}$ is thermodynamically favored by the abundance of the reactants, dissolved calcium ($[Ca^{2+}]$), and carbonate ($[CO_3^{=}]$) ions. While oceanic $[Ca^{2+}]$ is relatively constant at high levels that are well described by conservative relationships with salinity, ocean $[CO_3^{=}]$ decreases as atmospheric CO_2 rises, lowering the energetic favorability of $CaCO_{3,s}$ formation. This energetic favorability is proportional to the saturation state, Ω, defined by

$$\Omega_f = \frac{[CO_3^{=}][Ca^{2+}]}{K_{sp,f}}$$

where the subscript f refers to the phase of the mineral being formed and $K_{sp,f}$ is the apparent thermodynamic solubility product of that phase. Precipitation is thermodynamically possible for $\Omega_f > 1$, and greater values of Ω_f correspond to greater energetic favorability for precipitation. Calcium carbonate exists in a variety of phases distinguished by crystal structure and associated contributions of contaminaxting elements. The most common phases are the low-magnesium phases calcite and aragonite and high-magnesium calcite. Aragonite is about twice as

* Corresponding author: bhales@coas.oregonstate.edu

soluble as calcite, and the solubility of high-Mg calcites increases with increased magnesium in the crystal lattice (Morse and Mackenzie 1990). Aragonite, in particular, plays an important role in the calcareous structures produced by corals, pteropods, and early life stages of larval oysters.

The $CaCO_3$ shell-forming bivalves, including oysters (Gazeau et al. 2007; Miller et al. 2009; Waldbusser et al. 2011), mussels (Gazeau et al. 2007; Thomsen et al. 2010), and clams (Green et al. 2009; Talmage and Gobler 2009; Waldbusser et al. 2010), show negative responses to lowered Ω values, even when those perturbations occur above the $\Omega = 1$ thermodynamic threshold for the minerals in question. Larval oysters appear to be particularly susceptible to the influences of ambient seawater chemistry, as they form their larval shell material out of the more soluble aragonite (Stenzel 1964) and only deposit less soluble calcite following settlement. Additionally, some studies indicate amorphous calcium carbonate (ACC) as an even more soluble mineral precursor (Weiss et al. 2002) during early stages of calcification, although other studies question the ubiquity of this finding (Mount et al. 2004; Kudo et al. 2010).

Regardless of exact calcification mechanisms, previous studies have shown that oyster larvae respond negatively to more acidic conditions. Kurihara et al. (2007) found a reduction in development success when *Crassostrea gigas* larvae were exposed to acidified conditions (pH = 7.4). Watson et al. (2009) exposed D-hinge (1-d-old) larvae of the Sydney rock oyster (*Saccostrea glomerata*) to a range of pH conditions (7.6–8.1) over a period of 10 d and showed a significant decline in the survival and growth of young larvae at lower pH. In a study starting with 5-d-old larvae, Miller et al. (2009) also showed a significant decrease in growth rate of *C. virginica* when exposed to lower pH conditions but relatively little effect on survival. Reduced larval growth of *C. virginica* in response to reduced pH was also found by Talmage and Gobler (2009), with negative effects on survival and metamorphosis also observed. Studies on adult bivalves have shown that net calcification was possible under more acidified conditions (Gazeau et al. 2007), and the ability to overcome dissolution increased with postlarval size (Waldbusser et al. 2010). Mineral polymorph, high energetic costs of early life history development, and the generally high mortality rates in larvae (Rumrill 1990) all suggest larvae will be the most susceptible developmental stage of marine bivalves.

On the North American Pacific coast, native populations of the oyster *Ostrea lurida* were unable to sustain extensive harvesting (White et al. 2009), and the commercial oyster industry there is supported primarily by cultivation of the nonnative *C. gigas*, which was introduced near the beginning of the 20th century but has limited naturally sustaining populations (Ruesink et al. 2005) because of cold in situ temperatures limiting reproduction of this species and low residence times of water and, consequently, planktonic larvae in many local estuaries (Banas et al. 2007). Therefore, the commercial oyster industry is dependent on hatcheries that rear larvae to settlement size before distributing them to the growers. In recent years, natural and hatchery larval production have been severely depressed in the Pacific Northwest, and a lack of sufficient "seed" has threatened an industry with a total economic value estimated at US$278 million as of 2009 (Pacific Coast Shellfish Growers Association 2010). Hatchery problems started in 2006, when high concentrations of the pathenogenic bacterium *Vibrio tubiashii* were observed, perhaps associated with high-nutrient, low-O_2 coastal upwelled waters (Grantham et al. 2004; Chan et al. 2008) mixing with warm late-summer bay waters (Elston et al. 2008). The Whiskey Creek Shellfish Hatchery in Netarts Bay on the northern Oregon coast ($\sim$ 45.4°N, 123.9°W) experienced high concentrations of *V. tubiashii* and difficulties in seed production (Elston et al. 2008). However, by the summer of 2008, bacterial monitoring indicated that pronounced mortality events often occurred in the absence of detectable *V. tubiashii*. On the other hand, these larval mortality events often coincided with strong coastal upwelling and the presence of seawater thermodynamically unstable with respect to aragonite in Netarts Bay.

Although the effects of ocean acidification have been forecast for nearly 30 yr (Feely and Chen 1982), the issue has only recently received community-wide interest with workshops (Fabry et al. 2009) and strategy documents (e.g., National Research Council 2010) completed in the last few years, along with development of large-scale international integrated projects (http://www.epoca-project.eu) and locally integrated observation networks (http://c-can.msi.ucsb.edu). As a result, the chemical signature and ecological effects of acidification have been under way long before adequate scientific monitoring and classical experimentation could sufficiently be put in place to resolve either the baseline or the mechanisms of ecosystem responses. Because of this known information deficiency, workshop reports (Fabry et al. 2009) have strongly recommended that the scientific community engage affected stakeholders and attempt to mine nontraditional data sources for relevant information.

In this study, we follow this recommendation by augmenting existing monitoring measurements with state-of-the-art carbonate chemistry validation to evaluate the response of *C. gigas* larvae, grown under otherwise optimal conditions at an affected commercial hatchery on the Oregon coast, to natural changes in carbonate chemistry associated with periodic seasonal upwelling during the summer of 2009.

Methods

Whiskey Creek Hatchery (WCH), a commercial shellfish hatchery and largest independent producer of oyster seed in the Pacific Northwest, is located in Netarts Bay, a small bay on the northern Oregon coast (Fig. 1). Netarts Bay is a lagoon-type estuary dominated by water inputs from the adjacent North Pacific Ocean, with equivalent mean depth and tidal amplitude ($\sim$ 2 m) and only minimal freshwater inputs via two small creeks that enter the east and south edges of the bay. The hatchery is situated on the eastern edge of the bay, about halfway between its northern and southern extents. Seawater for larval rearing is drawn

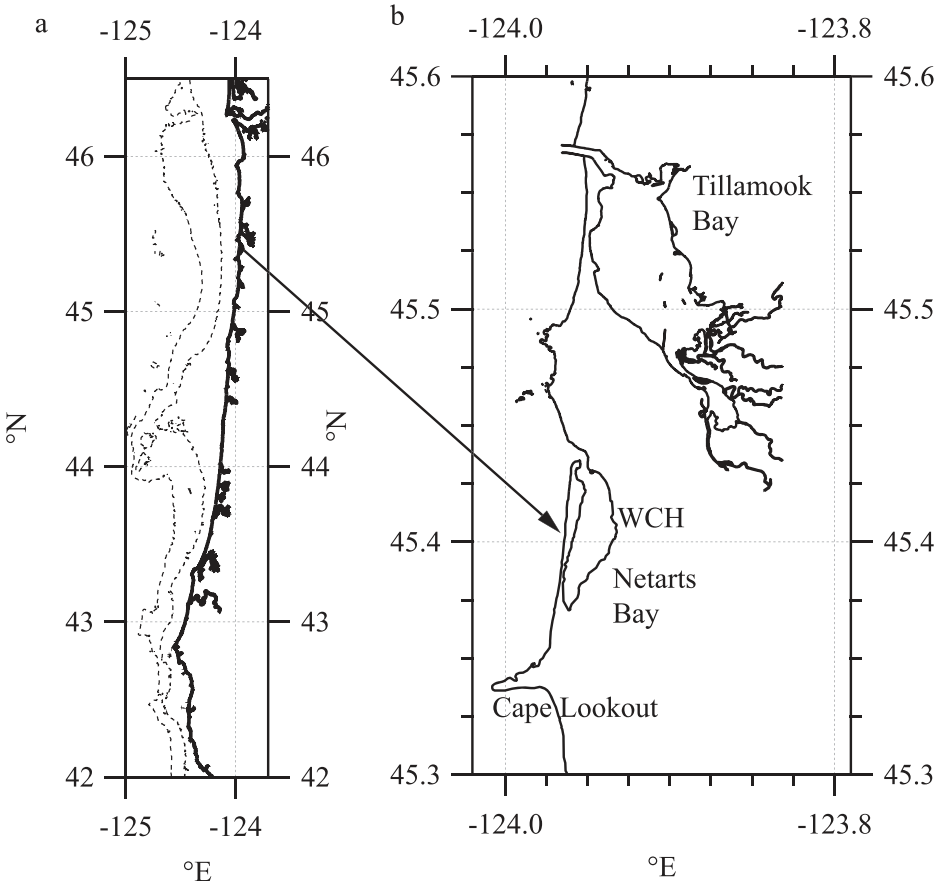

Fig. 1. (a) Map of Oregon coast from California border to the mouth of the Columbia River. Dotted contours offshore show the position of the 100- and 200-m isobaths. (b) Expanded view of Netarts Bay, where "WCH" denotes the position of the Whiskey Creek Hatchery.

directly from the bay through a submerged intake pipe about 0.5 m above the bottom at an average water depth of about 2 m. Temperature is maintained at either ~ 18°C (for broodstock) or ~ 25°C (for fertilization and larval rearing) within the hatchery, while salinity varies with natural fluctuations, in this case over a range of ~ 28–33.

The oyster production cycle within the hatchery follows general procedures for oyster hatchery production. Broodstock are obtained from sustaining native populations in Willapa Bay, Washington, oyster reserve or from the Molluscan Broodstock Program (http://hmsc.oregonstate.edu/projects/mbp/index.html) throughout the production cycle. After they are brought to the hatchery, they are kept in tanks flushed with ambient Netarts Bay seawater maintained at 18°C and fed with an excess supply of algae (produced in the hatchery) for a minimum of 2 wk to maximize fitness and fecundity while preventing natural spawning by not allowing temperatures to rise above 18°C. Oysters are strip spawned by sacrificing several individual males and females that are visually confirmed to be in peak fitness and fertility. Spawns are performed two to four times each week throughout the growing season, producing cohorts of 2×10^8–2×10^9 larvae per spawn.

Harvested eggs are screened to remove debris and thoroughly rinsed on a 20-μm screen. Clean eggs are resuspended in 0.1-m^3 tanks of filtered seawater, typically at concentrations of 10^{10} m^{-3}, then fertilized with a sperm suspension. Within 30–60 min, eggs are examined microscopically to insure proper fertilization and then placed into 22-m^3 tanks of seawater at concentrations not exceeding 2×10^7 m^{-3}. This represents one cohort of oyster larvae.

After 48 h, D-hinge larvae are collected during tank water change and transferred to 22-m^3 tanks of new seawater pumped from the bay; larvae are stocked initially at a concentration of 5×10^7 m^{-3}. Small larvae are fed a diet of the haptophyte *Isochrysis galbani* at cell densities of ~ 5×10^{10} m^{-3} until 7–10 days after fertilization. For the next few weeks, larvae are fed a mixed diet of diatoms (primarily *Chaetoceros gracilis* and *Thalassiosira* sp. fed at cell densities of ~ 7×10^{10} m^{-3}), and water in the holding tanks is replaced completely every 48 h. Larvae are typically large enough to be retained on 100-μm sieves (nominally 140–150 μm in long-axis shell length) within 1–2 wk after fertilization.

Although we do not discuss later development here, the hatchery produces and rears larvae until roughly 12–24 h before settlement, when they are packaged and shipped to commercial oyster growers across the Pacific Northwest. Rearing of successful cohorts continues for an additional 7–14 d beyond the times described above, at which point

larvae are harvested on 236-μm sieves (310–330-μm shell length) and distributed to growers. Low-production cohorts are not maintained beyond the 150-μm size threshold.

Hatchery operators have found that certain optimal ratios of biomass per volume are ideal for growth and feeding in various settings. In order to balance production rates and expenses associated with heating and maintain water, the hatchery maintains a near-constant tank-specific biomass by condensing or dividing cohorts into or across tanks as required. The hatchery uses a volumetric cone to estimate tank biomass and adjust the number of tanks as needed at each tank change. We can therefore utilize the data collected on the total number of tanks per cohort as a measure of larval biomass production. The change in the number of tanks is thus a proxy for the net production of a cohort of larvae. Relative larval production, P, was calculated from the relative change in the number of tanks between the initial number of tanks at the postfertilization D-hinge stage to the number of tanks when larvae are retained on 100-μm screens, that is, $P = (T_{100} - T_D)/T_D$, where T_{100} and T_D are the numbers of tanks at the 100-μm screen and D-hinge stages of production, respectively. A value of 0 in this case would imply no larval biomass production and could be attained by either limited growth and high survival or high growth and low survival, while a value of 1 would imply a doubling of larval biomass, and a value of -1 would imply complete mortality.

Hatchery personnel estimate larval development and growth by various metrics. Early development is tracked by estimating the number of fertilized eggs that develop to healthy D-hinged larvae as the ratio of healthy D-hinged larvae over successfully fertilized eggs. Growth is tracked by logging the number of days it takes for components of a cohort to reach benchmark sizes based on direct observations and sieves used to capture larvae during regular tank changes. Specifically, the number of days until the first observation of 120-μm larvae and the number of days until all surviving larvae reach 150 μm are cataloged. We utilized these records to estimate early-stage growth and midstage growth related to important transitions in larval feeding and development stages. Early-stage growth was defined as the time required until the first observation of individuals in a cohort reaching a shell length of 120 μm. Up to this size stage, sizes are obtained by microscopic analyses of subsamples from the cohort. Importantly, this metric potentially captures the dynamics of the fittest individuals in the cohort; however, the D-hinge developed integrates the entire early development. We defined midstage growth by calculating the time between first observation of larvae at 120-μm shell length and the time at which all surviving larvae are retained on a 100-μm screen (nominally 150-μm shell length). Larval nutrition in early-stage growth is reported to be mixotrophic with larvae depending on both egg reserves and limited ingestion of microalgae (Rico-Villa et al. 2009; Kheder et al. 2010*a,b*). In midstage growth, larvae become more dependent on exogenous food sources, and changes in diet or food availability have more pronounced effects on growth (Rico-Villa et al. 2009; Kheder et al. 2010*a,b*).

Water samples were collected from the hatchery seawater system weekly in the morning ($\sim$ 08:00 h local time) and afternoon (14:00 h) in addition to a few other times selected by the hatchery personnel. This sampling point was separated from the bay by a flow transit time of a few seconds and coincides with the location in the hatchery where the tanks are filled. Samples for analysis of seawater CO_2 partial pressure (P_{CO2}) and total dissolved CO_2 (T_{CO2}) were collected in 350-mL amber glass bottles with minimal headspace and poisoned with 300 μL of saturated $HgCl_2$ solution before being sealed with urethane-lined crimp-seal metal caps. We have shown in previous research (Hales et al. 2005; Bandstra et al. 2006) that samples collected in this manner are stable for several months or more for CO_2 analyses. Samples were analyzed for T_{CO2} following the method developed in Hales's lab by Bandstra et al. (2006) and for P_{CO2} by recirculating headspace air through the sample and a nondispersive infrared detector using a small air pump and a fritted bubbling stone. Results were corrected for the pressure of analysis headspace and for the temperature difference between analytical and in situ conditions to yield P_{CO2} values in dekapascals rather than the nearly numerically equivalent and more widely used μatm unit at in situ temperature (T) and T_{CO2} values in μmol kg^{-1}. Uncertainty for the T_{CO2} analyses is expected to be less than 0.2% (accuracy and precision), based on the results of Bandstra et al. (2006), and less than 5% for the P_{CO2} analyses, based on comparison between archived samples and measurements made in situ by a variety of methods (membrane and showerhead equilibration of flowing sample streams and moored measurement of P_{CO2} using absorbance-based sensors; Evans et al. 2011).

Inlet water aragonite saturation state (Ω_A) was calculated from the T, salinity (S), and P_{CO2} and T_{CO2} data at in situ conditions using a program written by the authors that accounts for the equilibrium interactions between the carbonic acid species at in situ conditions, using the carbonic acid dissociation constants of Mehrbach et al. (1973) as refit by Lueker et al. (2000), the boric acid constants as defined by Dickson (1990), and the aragonite solubility as defined by Mucci (1983). This choice of constants is appropriate for freshwater and salinities above 20 but is unverified for the range 0–20 and should be used with caution in lower salinity ranges where verification is insufficient. Calcium concentrations were calculated assuming conservative dependence on salinity with a freshwater end member of 1 mmol kg^{-1}, appropriate for local riverine inputs. From these measurements and choice of equilibrium constants, we can calculate pH on the total hydrogen ion scale, hereafter referred to as pH_T. Propagation of analytical uncertainty in the measured P_{CO2} and TCO_2 data (stated above) dominates the uncertainty in calculated Ω_A, which is about 5%, while calculated pH_T is uncertain by about $\pm$ 0.02. We do not consider inaccuracy in the thermodynamic constants used in our calculations. The most significant of these is the inaccuracy of the solubility of aragonite, which, as reported in the literature is uncertain by about $\pm$ 10%,. Absolute values of Ω_A and pH_T will suffer additional accuracy uncertainty if the equilibrium constants are considered, but relative changes in either term are known to within the above-stated propagation of analytical precision. Comparison of these

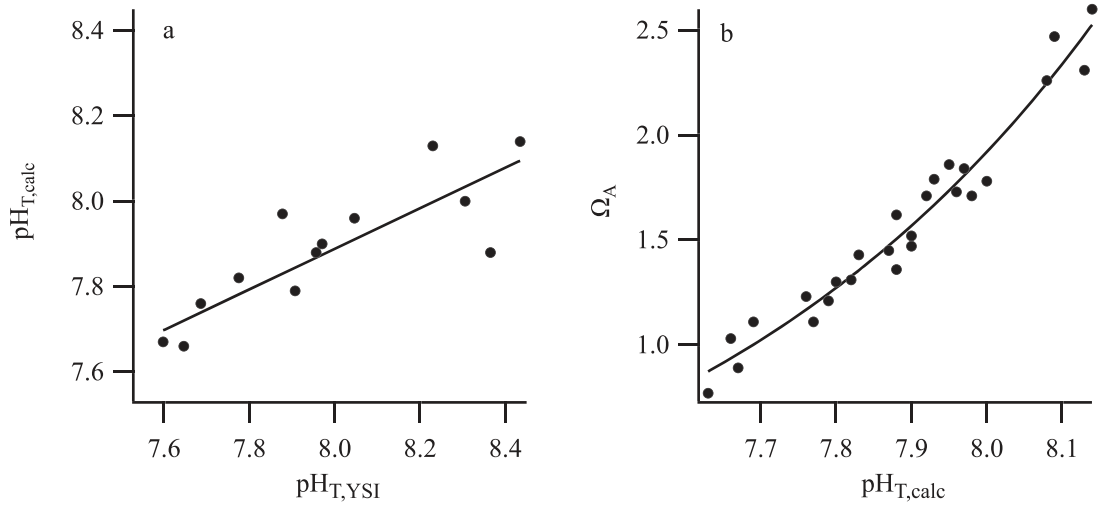

Fig. 2. (a) Correlation between $pH_{T,calc}$ calculated from P_{CO2} and T_{CO2} measured on discrete samples and $pH_{T,YSI}$, corrected to the total hydrogen ion scale from the NBS-scale pH measured with the YSI 6000 EDS sonde, for those samples with good T, S agreement. $pH_T = 0.45pH_{T,YSI} + 4.22$, $F_{1,12} = 26.80$, $p = 0.0002$, $R^2 = 0.70$. (b) Relationship between aragonite saturation state (Ω_A) and $pH_{T,calc}$ for all discrete samples ($\Omega_A = -0.288 + 0.9274e^{(1.7345\Delta pH_T)}$, $F_{2,23} = 248.84$, pseudo-$R^2 = 0.96$, $p < 0.0001$, where $\Delta pH_T = pH_T - 7.5$ and pseudo-$R^2 = 1 -$ [residual sums of squares divided by the total corrected sums of squares], appropriate for nonlinear regressions).

results with those of other studies will require careful examination of acid dissociation and mineral solubility assumptions.

It is important to note that the data presented here are for the conditions at the hatchery inlet sampling point. We maintain this for two reasons. Part of our objective is quantification of the natural variation in conditions in ambient bay waters, and direct measurements were not made in the water after heating. Treatment of the water approximates isochemical heating, in which alkalinity and T_{CO2} do not change because of the quiescent conditions and short time scale of the heating and the slow response of CO_2 to gas exchange. If waters were only warmed, calculated Ω_A values would be about 0.2 higher in warmed waters than at the intake at in situ T, and thus the responses we report would take place at more stable mineral solubility conditions. The most likely chemical change would be relaxation of the warmed waters to P_{CO2} values in equilibrium with the atmosphere while alkalinity remained constant. This would have two consequences. Warmed waters would mostly lose CO_2 to the atmosphere, resulting in potentially higher mean Ω_A values, and moving toward a common P_{CO2} would tend to reduce the dynamic range in Ω_A. Therefore, our measurements, if anything, underestimate the mean Ω_A and overestimate its dynamic range in fertilization and rearing waters. We believe that this choice of Ω_A values is the most conservative in implicating ocean acidification effects on larval oysters.

The high variability of the bay-water chemistry and the frequency of the spawning operations made the approximately weekly discrete samples alone insufficient for capturing the conditions experienced during spawning operations, and we were forced to use these discrete samples to ground-truth a continuous record of pH being recorded by an in situ Yellow Springs Instruments (YSI) 6000 EDS sonde, located in the bay at the inlet of the hatchery intake pipe, starting in late May 2009. Along with pH, the sonde also recorded temperature and salinity at 30-s intervals. The sonde was recovered monthly for cleaning and calibrated for pH using Oakton buffers (http://www.4oakton.com) at pH 7 and 10 on the National Bureau of Standards (NBS) scale. One calibration operation occurred in the middle of the presented record on 01 July 2009 and two others preceding and following the sampling interval. No drift was obvious during these calibrations, and no drift correction was applied.

As there can be decoupling between pH and mineral saturation state, pH is an imperfect variable for assessing corrosivity of ocean water to calcium carbonate biominerals. This is especially true in a complicated matrix like seawater where ionic strength effects can lead to large uncertainties in the determination of pH itself. We made two corrections to the in situ pH record. We first corrected the NBS-scale YSI measurements to the total hydrogen ion scale using the nonlinear empirical relationship between the total hydrogen ion activity coefficient and temperature and salinity given by Millero et al. (1988). The corrections made to adjust to the pH_T scale were on the order of 0.13 unit, with dependence on the T and S of the sample water. We then synchronized our discrete measurements with the continuous in situ record and used our calculated pH_T values to verify the accuracy of the in situ measurements. We limited our analyses only to times when the measured discrete sample T and S agreed with the synchronized in situ observations to within $\pm$ 0.5°C and 0.75, respectively, to ensure comparisons of common water types. The discrete and in situ T and S measurements were quite closely correlated ($R^2 > 0.98$ for both parameters), but periodic deviations occurred, as expected in a dynamic setting such as this. The linear relationship between in situ and discrete-sample calculated pH (Fig. 2a) was used to convert the continuous in situ record into one that was

internally consistent with our CO_2 chemical analyses ($pH_{T,calc} = 0.45pH_{T,YSI} + 4.22$, $F_{1,12} = 26.80$, $p = 0.0002$, $R^2 = 0.70$). This correction is large, with slope < 1 and offset > 0. This is not unexpected, as the YSI electrode is advertised to produce accuracy of only $\pm$ 0.2 unit, although precision is 0.01 unit (http://www.ysi.com/productsdetail.php?6600V2-1). If this inaccuracy exists as nonlinearity in relatively narrow pH ranges ($\sim$ 0.6 in this case) or as function of T and/or S fluctuations, none of which are specified by the manufacturer, it could account for the majority of this disagreement. However, the average residual difference between predicted pH_T from our regression analysis and measured pH_T is 0.06 ($\pm$ 0.06, 1 SD), with a maximum residual value of 0.19; thus, for our purposes, this is adequate.

As stated, pH is not expected to be a perfect predictor for mineral saturation state, but the correlation between pH_T and Ω_A from our discrete samples (Fig. 2b) was strong enough to give good predictive power ($\Omega_A = -0.288 + 0.927e^{(1.735\Delta pHt)}$, $F_{2,23} = 248.84$, pseudo-$R^2 = 0.96$, $p < 0.0001$, where $\Delta pH_T = pH_T - 7.5$ and pseudo-$R^2 = 1 -$ [residual sums of squares divided by the total corrected sums of squares], appropriate for nonlinear regressions). After correcting the in situ pH with the relationship shown in Fig. 2a, we then converted that record to a continuous time series of Ω_A with the relationship shown in Fig. 2b. Conditions for individual spawns were determined by averaging the Ω_A record between 0:800 h and 12:00 h local time on the day of the spawn, corresponding to the interval in which spawn tanks were filled.

A simple linear regression analysis was used to quantify the effect of aragonite saturation state at time of spawn on the proportion of healthy D-hinge, relative production value (both described above), the early-stage growth rate (up to 120-μm shell length), and the midstage growth rate (120–150-μm shell length). The proportional D-hinge data were arcsin square-root transformed because of the problems associated with parametric analysis of proportional data. Assumptions of heteroscedasticity and normality of residuals were checked with visual examination of residuals and by the Shapiro–Wilk statistic, and these assumptions were met. We additionally checked for overly influential data points by examining Studentized residuals and Cook's distance and found one observation that corresponded to an overly influential data point in two of the three regressions. We censored each point and repeated the statistical analyses but have included the point on subsequent graphs. The exclusion of this point did not change the inferences from either analysis. All analyses were run in SAS v9.1, using Proc Reg for linear regressions and Proc Nlin for the nonlinear regression.

Results

Netarts Bay carbonate chemistry—Water sampling and continuous analysis for the period 01 June–03 August 2009 (Figs. 3, 4) show that the bay is subjected to two major forcings that affect its carbonate chemistry. The first is the upwelling state of the adjacent coastal ocean. During upwelling, evidenced by high atmospheric pressure and strong north winds (Fig. 3a), colder, saltier (Fig. 3b), low-pH (Fig. 3c) aragonite-undersaturated (Fig. 3d) deep-origin upwelled water is brought to the surface very near the coast (Hales et al. 2005; Feely et al. 2008), and this water spills over the sill at the bay mouth into the bay. During reduced upwelling or relaxation events, low-CO_2 photosynthetically modified (high pH, high Ω_A) surface waters are forced back onshore and enter the bay. The time scale of this forcing ranges from several days, corresponding to the frequency of relaxation events during the upwelling season, to several months, corresponding to the seasonal shift between winter downwelling- and summer upwelling-favorable winds. During the record of interest in 2009, there were periods of strong upwelling from about year-day 161–186 (10 June–05 July) and again from about year-day 195–212 (14–31 July), punctuated by periods of weak variable to south winds from year-day 153–161 (02–10 June), 187–194 (06–13 July), and 213–217 (01–05 August).

The second forcing factor is diurnal metabolic variability within the bay. This is visible as the high-frequency patterns superimposed on the smoothed records of Fig. 3, and one part of the record is examined in more detail in Fig. 4. The bay contains broad shallows populated by extensive eelgrass beds and benthic microalgae, and on high-insolation days, photosynthetic uptake of CO_2 from bay waters is high. In contrast, nighttime respiration produces abundant CO_2. This results in a clear pattern of high P_{CO2} and T_{CO2} in the morning discrete samples, with greatly reduced levels in the afternoon samples (Fig. 4), that drives the diurnal signal in pH_T and Ω_A (e.g., increasing values during the day and decreasing values through the night). Note that thermal forcing alone would predict higher afternoon P_{CO2}, opposite of what is seen. This effect occurs independent of tidal forcing and is apparent in both upwelling and relaxation (or reversal) oceanic conditions. Unlike the upwelling-modulated changes, the bay's carbonate chemistry is decoupled from its temperature and salinity in these intervals.

Oyster larval performance—Larval performance was assessed by four measures derived from hatchery records: early development to D-hinge, the relative production, early-stage growth when larvae depend on mixotrophic nutrition, and midstage when larvae transition to exogenous food sources. Successful development from fertilized egg to D-hinge is measured by the proportion of fertilized eggs that make it to D-hinge in $\sim$ 24 h. The relative production term provides a proxy for cohort biomass, with positive numbers indicating growth in cohort biomass and negative numbers indicating mortality. Our early- and midstage growth metrics estimate the time required to reach and exceed a benchmark size. Aragonite saturation state at the time of spawning did not have significant effects on D-hinge development ($F_{1,14} = 3.97$, $p = 0.0663$, adjusted $R^2 = 0.17$; Fig. 5a) and early-stage growth ($F_{1,15} = 0.00$, $p = 0.9845$, adjusted $R^2 < 0$; Fig. 5b). However significant effects of carbonate conditions at time of spawn were found on midstage growth ($F_{1,14} = 13.87$, $p = 0.0025$, adjusted $R^2 = 0.47$; Fig. 5c) and relative production ($F_{1,15} = 17.93$, $p = 0.0008$, adjusted $R^2 = 0.53$; Fig. 5d). Differing numbers of

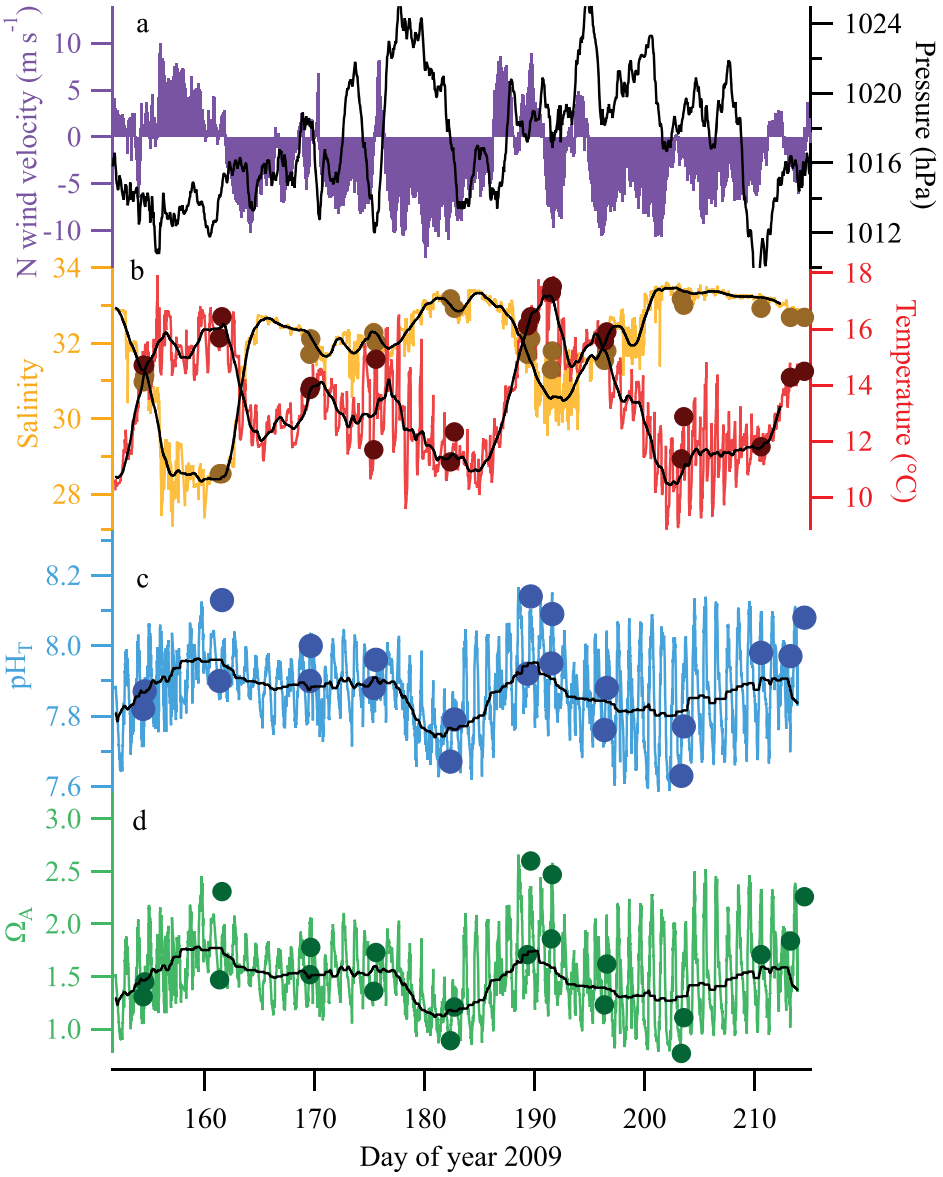

Fig. 3. Variability in environmental conditions in Netarts Bay, 01 June–03 August 2009. (a) Record of north wind velocity (left axis) and atmospheric pressure (right axis), showing the atmospheric conditions driving upwelling variability over the period of interest. (b) Record of salinity (left axis) and temperature (right axis) at the hatchery intake. Black lines are 3-day running-median smoothed representations of each record, distinguishing the upwelling forcing from the diurnal forcing. Similarly colored circles are corrected discrete measurements of each parameter, corresponding to the discrete samples analyzed for CO_2 chemistry. (c) pH_T from the corrected in situ measurements made by the YSI sonde at the hatchery intake (blue line) and calculated from the discrete samples analyzed for P_{CO2} and T_{CO2} (blue circles). Black line is the 3-day filtered pH_T record, as for T and S, above. (d) Aragonite saturation (Ω_A), calculated from the corrected YSI pH_T data and the regression of Fig. 2b (green line) and from the discrete measurements of P_{CO2} and T_{CO2} (green circles).

degrees of freedom result from either missing data points or one data point in each of the midgrowth and relative production regressions having been censored due to the finding that each point was overly influential by Studentized residuals, Cook's distance, and DFFITS diagnostics. These censored data points have, however, been included in the plots of Fig. 5 as filled circles.

Discussion

This work differs from previous studies of calcifying organism responses to changing acid-base chemistry in several key ways. First, we utilized hatchery records of larval performance under naturally fluctuating ambient-water CO_2 chemistry of Oregon's coastal upwelling system

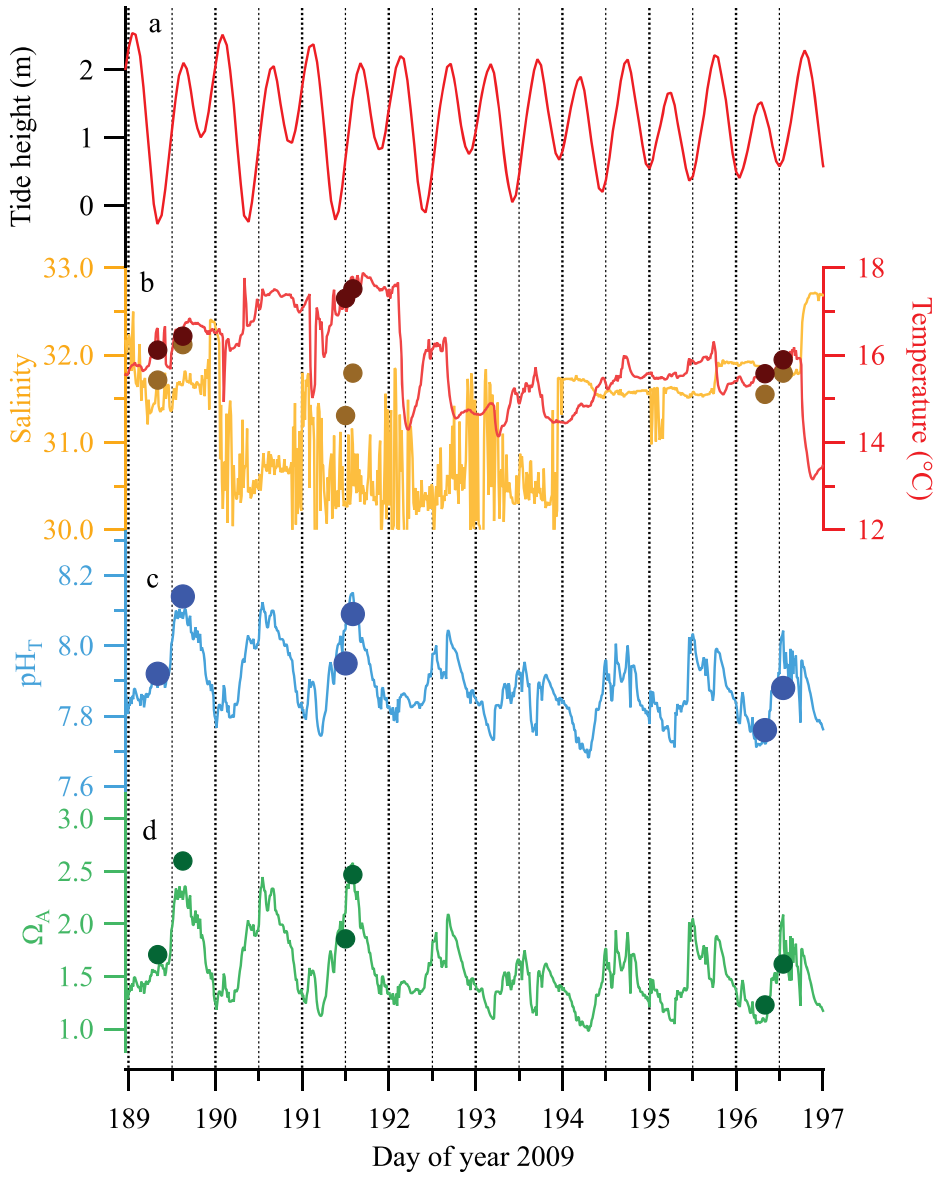

Fig. 4. Demonstration of effect of diurnal variability on Netarts Bay carbonate chemistry for a subset of the data presented in Fig. 3, 08–17 July 2009. (a) Tidal stage is largely uncorrelated with (b) in-bay T and S or (c) pH or (d) aragonite saturation. Bay carbonate chemistry shows regular diurnal variability, with maximum pH_T and Ω_A at or shortly after local noon and minima in early morning. Vertical dashed lines represent local midnight (major ticks) and noon (minor ticks).

with *C. gigas*, a nonnative study organism that has been resident in these waters for nearly a century. No artificial manipulations of water chemistry outside of those occurring naturally were conducted. Second, we have focused on the larval stages of several cohorts grown under commercial hatchery conditions and protocols. Finally, we have resolved the vagaries of in situ pH electrode time-series data with discrete measures of seawater carbonate chemistry analyzed with state-of-the-art methodology. With this novel approach, we have observed significant relationships between aragonite saturation states at the time of spawning and subsequent growth and production of larvae over the size range of ~ 120 to ~ 150-μm shell length (Fig. 5) but not on early growth and development.

Recent work by A. Hettinger (unpubl.) on the native *O. lurida* showed carryover effects of water chemistry experienced at early stage (larvae) to the later postlarval juvenile stage. The carryover effect was evident after 1 mo of growth when juveniles exposed to acidified conditions in their larval stages failed to attain the same size as juveniles derived from larvae exposed to less acidic conditions. Our findings and those of A. Hettinger (unpubl.) illustrate important concepts of how variable acidification may affect coastal and estuarine ecosystems. The timing of spawning

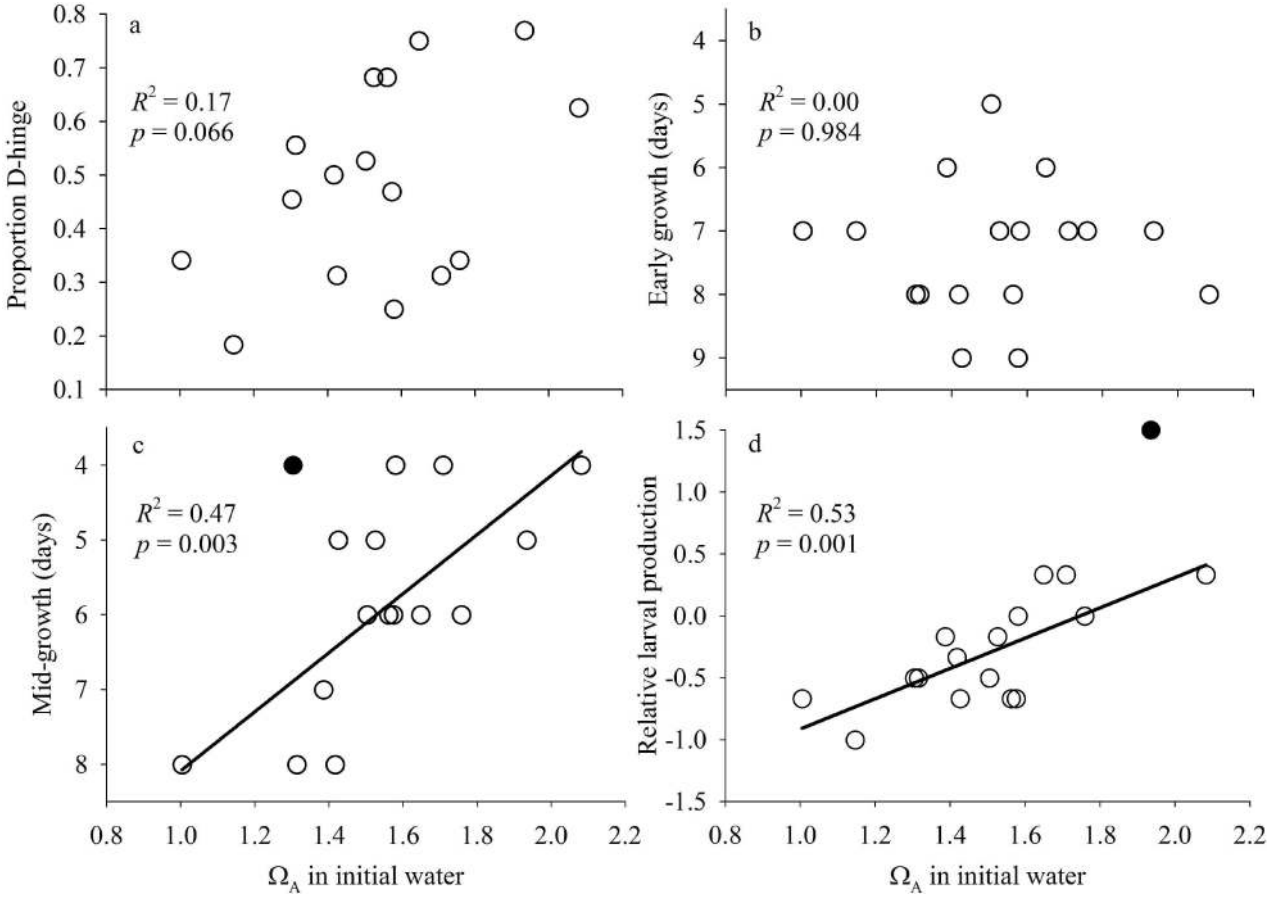

Fig. 5. Relationship between saturation state of aragonite and (a) proportion of larvae developing to D-hinge stage, (b) number of days for larvae to reach a nominal 120-μm size, (c) number of days for larvae to grow from 120- to 150-μm nominal size, and (d) overall relative production of each cohort. As described in the Methods section, relative production does not include the changes in the cohort prior to D-hinge; relative production captures only the changes from the D-hinge stage up to competent to settle. Data points in black on graphs 5c and 5d are statistical outliers and were excluded from regression analysis. Reduced R^2 values and p-values of linear regression analyses are shown in the figure. Other statistics for significant relationships are (c) midstage, growth slope = -3.95 ± 1.05 days, intercept = 12.02 ± 1.67 days and (d) relative production, slope = 1.22 ± 0.29 days, intercept = -2.13 ± 0.44 days.

and release of gametes into the water column are critical in light of variable local conditions occurring on top of a shifting CO_2 chemistry baseline (Waldbusser et al. 2010, 2011). Others have demonstrated the importance of environmental conditions related to climate and weather patterns in controlling interannual oyster recruitment (Kimmel and Newell 2007). Our results further highlight the ecological significance of windows of opportunity for successful recruitment that may be likened to match–mismatch theory (Cushing 1990). However, it is important to note that in the current study, we have evaluated hatchery production and therefore minimized the typically extreme mortality of larval oysters in the wild by growing them under otherwise ideal conditions.

Long-term records of recruitment of Pacific oysters in Willapa Bay, Washington, have previously shown multiple year failures in recruitment (Dumbauld et al. 2011). Recent Pacific Northwest failures in natural recruitment have also corresponded with diminished oyster seed production at WCH (S. Cudd pers. comm.). Within a hatchery setting, oysters are spawned frequently (every few days at WCH over several months) and cohorts distinct, whereas natural populations typically have fewer cohorts per season that are often variable in timing and generally result in an integrated cohort over the spawning season. Within the hatchery, temperature and food concentrations are all held at near-constant and optimal levels, and broodstock are optimized for reproduction, while these conditions vary significantly in natural waters during the spawning season. Additionally, Rumrill (1990) noted that fertilization failure, adverse hydrography, substrate limitation, and predation are the most important determinants of the success of natural populations of meroplankton, such as larval oysters. Recent biochemical studies of oyster larvae indicate the importance of food quality and quantity in conjunction with sensitivity to fluctuating salinity and temperature (Hofmann et al. 2004). Increased food availability and quality generally improved tolerance of *C. gigas* larvae to salinity and temperature variability in these modeling studies. If we view the less favorable aragonite formation energetics associated with high-CO_2 upwelling conditions as sublethal acute stress and recognize

that early development is energetically expensive, as is shell construction (Palmer 1992), then the moderate acidification we measured can be considered a stress that requires additional energy to overcome (Portner 2008).

Many marine bivalve species share similar developmental stages from egg fertilization to metamorphosed juveniles, although the timing and typical sizes at which these stages occur will vary both within and among species. Recent studies suggest that early *C. gigas* larvae up to about 120 microns in shell length are mixotrophic, with egg yolk reserves providing a major source of nutrition (Rico-Villa et al. 2009; Kheder et al. 2010*a,b*). In our analyses of production and growth, there was no significant Ω_A effect (over the natural range of conditions) during early egg development on growth through this early stage (Fig. 5a,b); however, production was ultimately affected (Fig. 5d). This finding suggests that within-cohort variability may allow some individuals to continue to grow without incident while reaching our initial early-growth benchmark (Fig. 5b), while others cannot survive, leading to increased mortality and ultimately decreased cohort production (Fig. 5d). It is important to note that the relative production term uses the change in number of tanks from the D-hinge stage to competent to settle and therefore does not overlap with the proportion of D-hinge value. Growth was, however, significantly affected for midstage larvae that depend primarily on exogenous food sources (Fig. 5c). These findings suggest that the effects of acidification during egg development may have carried over (A. Hettinger unpubl.) to affect the growth and survival of midstage larvae. The nature of this putative carryover effect is unclear but could be due to the cumulative effects of stress on later larval development, metabolism or feeding physiology. Further research on the effects of ocean acidification on larval development and physiology is needed.

The fact that the bay itself experiences large fluctuations in carbonate chemistry driven by primarily natural mechanisms provides an opportunity for adaptive strategies to be implemented by resource managers such as hatchery operators. In the case of Netarts Bay, WCH operators have already implemented a strategy to avoid early morning tank-filling operations during strong upwelling conditions and as a result have restored a significant amount of lost production. Nevertheless, climatic shifts that are likely to move the mean state toward higher-CO_2, more corrosive conditions are a cause for concern (Feely et al. 2009; Rykaczewski and Dunne 2010). Feely et al. (2008) estimated that the most recent exposure of upwelled source waters off the US west coast was a few decades ago, yet the waters were still influenced by addition of anthropogenic CO_2 from a 1960s-vintage atmosphere. If correct, this means that waters already in transit to the upwelling locations have been exposed to more recent, higher-CO_2 atmospheres, and increasingly corrosive upwelled water is inevitable in coming years. Likewise, the intensity and persistence of upwelling that has accompanied hypoxic events (Grantham et al. 2004; Chan et al. 2008) off the Oregon coast has been hypothesized as a recurring feature of a warming climate (Barth et al. 2007; McGregor et al. 2007). Enhanced upwelling will carry increased corrosivity of shelf waters, much as it drives increased hypoxia. In each case, the fluctuations in local CO_2 chemistry will be superimposed on a trend of increasing corrosivity, meaning that the conditions favorable for larval oyster production will have lower frequency of occurrence and shorter persistence. Even if commercial shellfish producers are able to predict favorable conditions, the windows of opportunity for these adaptive strategies to be implemented will be diminished.

Two significant shortcomings exist with regard to understanding acidification effects on natural populations of organisms in variable coastal and estuarine habitats: prediction of how carbonate conditions will vary in coastal and estuarine environments with increasing atmospheric CO_2 and a better understanding of the fundamental biology underlying the responses of multicellular organisms to acidification. The first of these will be addressed by development of better predictive capability (Juranek et al. 2009) such that stakeholders may be able to plan production operations for the most favorable conditions. Our limited experience suggests that the multitude of forcing time scales still requires high-resolution monitoring of water CO_2 chemistry before we are fully capable of developing predictive models.

The second can be addressed only by more focused experimental work on physiological mechanisms of early larval response in conditions with tightly controlled carbonate chemistry. Our findings in the hatchery setting corroborate the laboratory-based experiments of Kurihara et al. (2007) illustrating the sensitivity of the very early developmental stages to ambient chemistry, although the hatchery larvae in this study experienced a much narrower range of carbonate chemistry. The descriptive biology of oyster larvae has been well documented; however, the dynamic responses of initial shell formation to environmental signals is still poorly understood. Initial shell is thought to be formed between the periostracum and the shell gland and thus ''protected'' from ambient conditions. How protected this initial shell material is, the energetics of this initial shell formation, and physiological plasticity are still poorly constrained. Numerous studies have now illustrated a pattern of negative response to acidification for many marine species, including bivalves (Kurihara et al. 2007; Miller et al. 2009; Watson et al. 2009), and many more will likely follow. In almost all cases, it has been shown that mollusks tend to respond negatively to increasing corrosiveness of water. However, only a handful of studies have addressed the underlying physiological and ecological mechanisms of these responses to develop a clear and well-founded argument for how other related organisms will respond (Wood et al. 2008; Thomsen et al. 2010; Ries 2011). Although shell mineralogy is a possible first-order explanation for the responses of calcifying organisms to acidification (Cooley and Doney 2009), it is clear that many other factors will determine susceptibility of biogenic minerals to dissolution (e.g., Glover and Kidwell 1993), and calcifying organisms may respond in less predictable ways (Ries et al. 2009). Although the history of studies of biomineralization spans several decades, aspects of the mechanisms of shell formation are still poorly understood, in particular during the very early life stages of mollusks. Some

recent work questions our current understanding of biomineralization (Mount et al. 2004), and we are far from understanding the processes underlying the patterns of response.

The fact that multiple parameters in the CO_2 chemistry system (pH, P_{CO2}, Ω_A, and so on) all change in response to perturbations complicates this understanding, as there are very likely differential effects of these variables on different physiological processes. Experimental methods that can elucidate these mechanisms will be important. Finally, the ability to predict the acute and chronic sensitivities of organisms to high-CO_2 waters should be a goal of future research. There has been some suggestion that larval and juvenile organisms need to reach critical development states where they can compensate for the deleterious effects of elevated CO_2 levels (Green et al. 2009; Waldbusser et al. 2010), and it may be that *C. gigas* larvae are especially sensitive to chemical conditions at the time of spawning. This may require development of acute and chronic threshold definitions, assessment of the sensitivity of organisms to the persistence of conditions, and stage-based models of organism responses.

The current study illustrates the value of monitoring efforts, which, if applied with stakeholder interests at hand, can provide valuable economic feedback (as is the case with WCH). Our study, relying on hatchery records and utilizing their production model, does potentially suffer from the lack of strict control as found in other more constrained experimental systems. We therefore acknowledge the correlative and suggestive nature of this study; however, it highlights the significance of current-day variable carbonate chemistry effects on commercially important species (and reliant regional economy) in surface waters and validates previous laboratory-based acidification experiments in which carbonate chemistry was manipulated. The significant effects on hatchery-based oyster production indicates that local and regional acidification effects are already on us, and responses of these coupled natural human systems to increasing CO_2 are likely unfavorable.

Acknowledgments

We thank Sue Cudd and Mark Wiegert, owners and operators of the Whiskey Creek Hatchery, for their assistance with developing a sampling program at the hatchery and for sharing their operational and production data with us. This work was supported by the Pacific Shellfish Institute, through efforts led by Andrew Suhrbier, and the Pacific Coast Shellfish Growers Association, through efforts led by Robin Downey. Conversations with Alan Trimble were greatly instructive in building our understanding of the local shellfish environment and ecology. National Science Foundation grant OCE-1041267 supported G.G.W., and the National Oceanic and Atmospheric Administration Ocean Acidification Program supported R.A.F. in preparation of this manuscript. Pacific Marine Environmental Laboratory contribution number 3720. Two anonymous reviewers provided thoughtful comments that greatly improved the final manuscript.

References

Aydin, K. Y., G. A. McFarlane, J. R. King, B. A. Megreya, and K. W. Myers. 2005. Linking oceanic food webs to coastal production and growth rates of Pacific salmon (*Oncorhynchus* spp.), using models on three scales. Deep-Sea Res. II **52:** 757–780, doi:10.1016/j.dsr2.2004.12.017

Banas, N. S., B. M. Hickey, J. A. Newton, and J. L. Ruesink. 2007. Tidal exchange, bivalve grazing, and patterns of primary production in Willapa Bay, Washington, USA. Mar. Ecol. Prog. Ser. **341:** 123–129, doi:10.3354/meps341123

Bandstra, L., B. Hales, and T. Takahashi. 2006. High-frequency measurement of seawater total carbon dioxide. Mar. Chem. **100:** 24–38, doi:10.1016/j.marchem.2005.10.009

Barth, J. A., and others. 2007. Delayed upwelling alters nearshore coastal ocean ecosystems in the northern California current. Proc. Natl. Acad. Sci. **10:** 3719–3724, doi:10.1073/pnas.0700462104

Chan, F., J. A. Barth, J. Lubchenco, A. Kirincich, H. Weeks, W. T. Peterson, and B. A. Menge. 2008. Emergence of anoxia in the California current large marine ecosystem. Science **319:** 920, doi:10.1126/science.1149016

Cooley, S. R., and S. C. Doney. 2009. Anticipating ocean acidification's economic consequences for commercial fisheries. Environ. Res. Lett. **4:** 024007, doi:10.1088/1748-9326/4/2/024007

Cushing, D. H. 1990. Plankton production and year-class strength in fish populations—an update of the match-mismatch hypothesis. Adv. Mar. Biol. **26:** 249–293, doi:10.1016/S0065-2881(08)60202-3

Dickson, A. G. 1990. Thermodynamics of the dissociation of boric acid in synthetic seawater from 273.15 to 298.15 K. Deep-Sea Res. **37:** 755–766.

Dumbauld, B. R., B. E. Kauffman, A. Trimble, and J. L. Ruesink. 2011. The Willapa Bay oyster reserves in Washington state: Fishery collapse, creating a sustainable replacement, and the potential for habitat conservation and restoration. J. Shellfish Res. **30:** 71–83, doi:10.2983/035.030.0111

Elston, R. A., H. Hasegawa, K. L. Humphrey, I. K. Polyak, and C. C. Hase. 2008. Re-emergence of *Vibrio tubiashii* in bivalve shellfish aquaculture: Severity, environmental drivers, geographic extent and management. Dis. Aquat. Org. **82:** 119–134, doi:10.3354/dao01982

Evans, W., B. Hales, and P. Strutton. 2011. The seasonal cycle of surface ocean pCO_2 on the Oregon shelf, J. Geophys. Res. Oceans **116:** C05012, doi:10.1029/2010JC006625

Fabry, V. J., and others. 2009. Present and future impacts of ocean acidification on marine ecosystems and biogeochemical cycles. Report of the Ocean Carbon and Biogeochemistry Scoping Workshop on Ocean Acidification Research (UCSD, Scripps Institution of Oceanography; 9–11 October 2007).

Feely, R. A., and C.-T. A. Chen. 1982. The effect of excess CO_2 on the calculated calcite and aragonite saturation horizons in the northeast Pacific Ocean. Geophys. Res. Lett. **9:** 1294–1297, doi:10.1029/GL009i011p01294

———, S. C. Doney, and S. R. Cooley. 2009. Ocean acidification: Present conditions and future changes in a high-CO_2 world. Oceanography **22:** 36–47, doi:10.5670/oceanog.2009.95

———, C. L. Sabine, J. M. Hernandez-Ayon, D. Ianson, and B. Hales. 2008. Evidence for upwelling of corrosive "acidified" water onto the continental shelf. Science **320:** 1490–1492, doi:10.1126/science.1155676

Gazeau, F., C. Quiblier, J. M. Jansen, J. P. Gattuso, J. J. Middelburg, and C. H. R. Heip. 2007. Impact of elevated CO_2 on shellfish calcification. Geophys. Res. Lett. **34:** L07603, doi:10.1029/2006GL028554

Glover, C. P., and S. M. Kidwell. 1993. Influence of organic matrix on the postmortem destruction of molluscan shells. J. Geol. **101:** 729–747, doi:10.1086/648271

Grantham, B. A., and others. 2004. Upwelling-driven nearshore hypoxia signals ecosystem and oceanographic changes in the northeast Pacific. Nature **429:** 749–754, doi:10.1038/nature02605

Green, M. A., G. G. Waldbusser, S. L. Reilly, K. Emerson, and S. O'Donnell. 2009. Death by dissolution: Sediment saturation state as a mortality factor for juvenile bivalves. Limnol. Oceanogr. **54:** 1037–1047, doi:10.4319/lo.2009.54.4.1037

Hales, B., T. Takahashi, and L. Bandstra. 2005. Atmospheric CO_2 uptake by a coastal upwelling system Glob. Biogeochem. Cycles **19:** GB1009, doi:10.1029/2004GB002295

Hall-Spencer, J. M., and others. 2008. Volcanic carbon dioxide vents show ecosystem effects of ocean acidification. Nature **454:** 96–99, doi:10.1038/nature07051

Hofmann, E. E., E. N. Powell, E. A. Bochenek, and J. A. Klinck. 2004. A modelling study of the influence of environment and food supply on survival of *Crassostrea gigas* larvae. ICES J. Mar. Sci. **61:** 596–616, doi:10.1016/j.icesjms.2004.03.029

Juranek, L. W., and others. 2009. A novel method for determination of aragonite saturation state on the continental shelf of central Oregon using multi-parameter relationships with hydrographic data. Geophys. Res. Lett. **37:** L01601, doi:10.1029/2009GL040423

Kheder, R. B., C. Quere, J. Moal, and R. Robert. 2010*a*. Effect of nutrition on *Crassostrea gigas* larval development and the evolution of physiological indices. Part A: Quantitative and qualitative diet effects. Aquaculture **305:** 165–173, doi:10.1016/j.aquaculture.2010.04.022

———, ———, ———, and ———. 2010*b*. Effect of nutrition on *Crassostrea gigas* larval development and the evolution of physiological indices. Part B: Effects of temporary food deprivation. Aquaculture **308:** 174–182, doi:10.1016/j.aquaculture.2010.08.030

Kimmel, D. G., and R. I. E. Newell. 2007. The influence of climate variation on eastern oyster (*Crassostrea virginica*) juvenile abundance in Chesapeake Bay. Limnol. Oceanogr. **52:** 959–965, doi:10.4319/lo.2007.52.3.0959

Kudo, M., J. Kameda, K. Saruwatari, N. Ozaki, K. Okano, H. Nagasawa, and T. Kogure. 2010. Microtexture of larval shell of oyster, *Crassostrea nippona*: A FIB-TEM study. J. Struct. Biol. **169:** 1–5, doi:10.1016/j.jsb.2009.07.014

Kurihara, H., S. Kato, and A. Ishimatsu. 2007. Effects of increased seawater pCO_2 on early development of the oyster *Crassostrea gigas*. Aquat. Biol. **1:** 91–98, doi:10.3354/ab00009

Lueker, T. J., A. G. Dickson, and C. D. Keeling. 2000. Ocean pCO_2 calculated from dissolved inorganic carbon, alkalinity, and equations for *K*1 and *K*2: Validation based on laboratory measurements of CO_2 in gas and seawater at equilibrium. Mar. Chem. **70:** 105–119, doi:10.1016/S0304-4203(00)00022-0

McGregor, H. V., M. Dima, H. W. Fischer, and S. Mulitza. 2007. Rapid 20th-century increase in coastal upwelling off northwest Africa. Science **315:** 637–639, doi:10.1126/science.1134839

Mehrbach, C., C. H. Culberson, J. E. Hawley, and R. M. Pytkowicz. 1973. Measurement of the apparent dissociation constants of carbonic acid in seawater at atmospheric pressure. Limnol. Oceanogr. **18:** 897–907, doi:10.4319/lo.1973.18.6.0897

Miller, A. W., A. C. Reynolds, C. Sobrino, and G. F. Riedel. 2009. Shellfish face uncertain future in high CO_2 world: Influence of acidification on oyster larvae calcification and growth in estuaries. PLoS ONE **4:** e5661, doi:10.1371/journal.pone.0005661

Millero, F. J., T. Plese, and M. Fernandez. 1988. The dissociation of hydrogen sulfide in seawater. Limnol. Oceanogr. **33:** 269–274, doi:10.4319/lo.1988.33.2.0269

Morse, J. W., and F. T. Mackenzie. 1990. Geochemistry of sedimentary carbonates. Developments in Sedimentology 48. Elsevier.

Mount, A. S., A. P. Wheeler, R. P. Paradkar, and D. Snider. 2004. Hemocyte-mediated shell mineralization in the eastern oyster. Science **304:** 297–300, doi:10.1126/science.1090506

Mucci, A. 1983. The solubility of calcite and aragonite in seawater at various salinities, temperatures, and 1 atmosphere total pressure. Am. J. Sci. **238:** 780–799, doi:10.2475/ajs.283.7.780

National Research Council. 2010. Ocean acidification: A national strategy to meet the challenges of a changing ocean. National Academies Press.

Pacific Coast Shellfish Growers Association. 2010. Shellfish production on the west coast. Available from http://www.pcsga.org/pub/farming/production_stats.pdf

Palmer, A. R. 1992. Calcification in marine mollusks—how costly is it? Proc. Natl. Acad. Sci. **89:** 1379–1382, doi:10.1073/pnas.89.4.1379

Portner, H. O. 2008. Ecosystem effects of ocean acidification in times of ocean warming: A physiologist's view. Mar. Ecol. Prog. Ser. **373:** 203–217, doi:10.3354/meps07768

Rico-Villa, B., S. Pouvreau, and R. Robert. 2009. Influence of food density and temperature on ingestion, growth and settlement of Pacific oyster larvae, *Crassostrea gigas*. Aquaculture **287:** 395–401, doi:10.1016/j.aquaculture.2008.10.054

Ries, J. B. 2011. A physiochemical framework for interpreting the biological calcification response to CO_2-induced ocean acidification. Geochim. Cosmochim. Acta **14:** 4053–4064, doi:10.1016/j.gca.2011.04.025

———, A. L. Cohen, and D. C. McCorkle. 2009. Marine calcifiers exhibit mixed responses to CO_2-induced ocean acidification. Geology **37:** 1131–1134, doi:10.1130/G30210A.1

Ruesink, J. L., H. S. Lenihan, A. C. Trimble, K. W. Heiman, F. Micheli, J. E. Byers, and M. C. Kay. 2005. Introduction of non-native oysters: Ecosystem effects and restoration implications. Annu. Rev. Ecol. Evol. Syst. **36:** 643–689, doi:10.1146/annurev.ecolsys.36.102003.152638

Rumrill, S. S. 1990. Natural mortality of marine invertebrate larvae. Ophelia **32:** 163–198.

Rykaczewski, R. R., and J. P. Dunne. 2010. A measured look at ocean chlorophyll trends. Nature **472:** E5–E6, doi:10.1038/nature09952

Sabine, C. L., R. A. Feely, R. Wanninkhof, T. Takahashi, S. Khatiwala, and G.-H. Park. 2011. The global ocean carbon cycle. p. S100–S108. *In* State of the Climate in 2010, 3. Glob. Oceans. Bull. Am. Meteorol. Soc. **92:** S100–S108, doi:10.1175/1520-0477-92.6.S1

Steinacher, M., F. Joos, T. L. Frolicher, G. K. Plattner, and S. C. Doney. 2009. Imminent ocean acidification in the Arctic projected with the NCAR global coupled carbon cycle-climate model. Biogeosciences **6:** 515–533, doi:10.5194/bg-6-515-2009

Stenzel, H. B. 1964. Oysters: Composition of the larval shell. Science **145:** 155–156, doi:10.1126/science.145.3628.155

Talmage, S. C., and C. J. Gobler. 2009. The effects of elevated carbon dioxide concentrations on the metamorphosis, size, and survival of larval hard clams (*Mercenaria mercenaria*), bay scallops (*Argopecten irradians*), and eastern oysters (*Crassostrea virginica*). Limnol. Oceanogr. **54:** 2072–2080, doi:10.4319/lo.2009.54.6.2072

Thomsen, J., and others. 2010. Calcifying invertebrates succeed in a naturally CO_2-rich coastal habitat but are threatened by high levels of future acidification. Biogeosciences **7:** 3879–3891, doi:10.5194/bg-7-3879-2010

Waldbusser, G. G., H. Bergschneider, and M. A. Green. 2010. Size-dependent pH effect on calcification in post-larval hard clam *Mercenaria* spp. Mar. Ecol. Prog. Ser. **417:** 171–182, doi:10.3354/meps08809

———, E. P. Voigt, H. Bergschneider, M. A. Green, and R. I. E. Newell. 2011. Biocalcification in the eastern oyster (*Crassostrea virginica*) in relation to long-term trends in Chesapeake Bay pH. Estuar. Coasts **34:** 221–231, doi:10.1007/s12237-010-9307-0

Watson, S-A., P. C. Southgate, P. A. Tyler, and L. S. Peck. 2009. Early larval development of the Sydney rock oyster *Saccostrea glomerata* under near-future predictions of CO_2-driven ocean acidification. J. Shellfish Res. **28:** 431–437, doi:10.2983/035.028.0302

Weiss, I. M., N. Tuross, L. Addadi, and S. Weiner. 2002. Mollusc larval shell formation: Amorphous calcium carbonate is a precursor phase for aragonite. J. Exp. Zool. **293:** 478–491, doi:10.1002/jez.90004

White, J., J. L. Ruesink, and A. C. Trimble. 2009. The nearly forgotten oyster: *Ostrea lurida* Carpenter 1864 (Olympia oyster) history and management in Washington State. J. Shellfish Res. **28:** 43–49, doi:10.2983/035.028.0109

Wood, H. L., J. I. Spicer, and S. Widdicombe. 2008. Ocean acidification may increase calcification rates, but at a cost. Proc. R. Soc. B Biol. Sci. **275:** 1767–1773, doi:10.1098/rspb.2008.0343

Associate Editor: John Albert Raven

Received: 17 May 2011
Accepted: 16 January 2012
Amended: 27 January 2012